ELSEVIER

Journal of Organometallic Chemistry 632 (2001) 67–74

Journal of Organometallic Chemistry

www.elsevier.com/locate/jorganchem

Synthesis, structural and magnetic characterization of the metamagnet $[Fe(C_5Me_5)_2]$DMe–DCNQI

S. Rabaça [a], R. Meira [a], L.C.J. Pereira [a], M. Teresa Duarte [b], V. da Gama [a,*]

[a] *Departament Química, Instituto Tecnológico e Nuclear, P-2686-953 Sacavém, Portugal*
[b] *Departament Engenharia Química, Instituto Superior Técnico, P-1049-001 Lisbon, Portugal*

Received 20 February 2001; accepted 29 March 2001

On the occasion of Professor A.R. Dias' 60th birthday.

Abstract

The addition of a solution of decamethylferrocene, $[Fe(Cp^*)_2]$, to a solution containing N,N′-dicyano-2,5-dimethyl-1,4-benzoquinonediimine, DMe–DCNQI, results in the formation of the electron-transfer salt $[Fe(Cp^*)_2]$DMe–DCNQI. A single crystal X-ray structure determination showed that this compound belongs to the triclinic space group $P\bar{1}$, with $a = 8.6665(6)$ Å, $b = 9.5552(5)$ Å, $c = 9.8392(5)$ Å, $\alpha = 101.421(5)°$, $\beta = 112.523(5)°$, $\gamma = 106.639(6)°$, $Z = 1$, $R_1 = 0.0536$, $wR_2 = 0.1499$. The solid state structure consists of an array of parallel alternating donors, $[Fe(Cp^*)_2]^{\bullet+}$, and acceptors, DMe–DCNQI$^{\bullet-}$, ···DADADA··· stacks along [111]. At high temperatures ($T > 20$ K), the magnetic susceptibility obeys to the Curie–Weiss expression, with a θ value of 3.2 K, revealing the existence of dominant FM interactions. At low temperatures a metamagnetic behavior was observed for $[Fe(Cp^*)_2]$DMe–DCNQI, with $T_N = 3.9$ K and $H_C = 5.5$ kG at 1.7 K, resulting from a high magnetic anisotropy, due to the coexistence of strong FM DA intrachain interactions and weaker AFM (DD and AA) interchain interactions.

Keywords: Magnetic molecular materials; Organometallic electron-transfer salts; Crystal structures; Metamagnetism; Decamethylferrocenium

---

1. Introduction

The observation of metamagnetism in the organometallic electron-transfer salt $[Fe(Cp^*)_2]$TCNQ [1] in 1979 was a landmark in the search for bulk molecule-based ferromagnets, which was reported for the first time in 1986 for $[Fe(Cp^*)_2]$TCNE [2], with a critical temperature, T_C, of 4.8 K. This discovery gave a significant impulse to the field of molecular magnetism and, since then, a considerable attention has been given to the study of these materials, in particular to the electron-transfer salts (ETS) based on decamethylmetallocenes and on planar acceptors [3,4]. Bulk ferromagnetism was reported for several ETS based on decamethylmetallocenes and on the conjugated polynitriles TCNE [2,5] and TCNQ [6] and metamagnetism was also observed in several decamethylmetallocene based ETS, with planar acceptors such as TCNQ [1] and metal-bis(dichalcogenate)

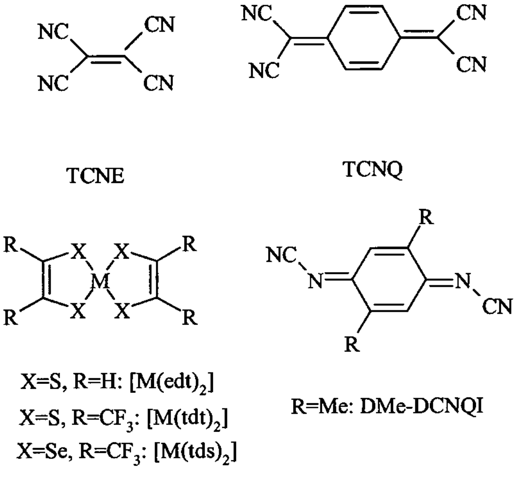

Scheme 1.

---

* Corresponding author. Tel.: +351-21-996-6203; fax: +351-21-994-1455.
E-mail address: vascog@itn.pt (V. da Gama).

PII: S0022-328X(01)00820-8

Table 1
Crystal data and structure refinement for [Fe(Cp*)$_2$]DMe–DCNQI

Empirical formula	$C_{30}H_{38}FeN_4$
Formula weight	510.5
Temperature (K)	293(2)
Wavelength (Å)	1.54178
Crystal system	Triclinic
Space group	$P\bar{1}$
Unit cell dimensions	
a (Å)	8.6665(6)
b (Å)	9.5552(5)
c (Å)	9.8392(7)
α (°)	101.421(5)
β (°)	112.523(5)
γ (°)	106.639(6)
V (Å^3)	676.14(8)
Z	1
D_{calc} (Mg m^{-3})	1.254
Absorption coefficient (mm^{-1})	4.646
F(000)	272
Crystal size (mm^3)	$0.50 \times 0.40 \times 0.20$
θ Range for data collection (°)	5.15–66.94
Index ranges	$-10 \leq h \leq 0$; $-10 \leq k \leq 11$; $-10 \leq l \leq 11$
Reflections collected	2549
Independent reflections	2388 [$R_{int} = 0.0677$]
Reflections observed ($>2\sigma$)	2233
Absorption correction	Psi-scans
Max. and min. transmission	0.99 and 0.47
Refinement method	Full-matrix least-squares on F^2
Data/restraints/parameters	2388/0/160
Goodness-of-fit on F^2	1.096
Final R indices [$I > 2\sigma(I)$]	$R_1 = 0.0536$ $wR_2 = 0.1427$
R indices (all data)	$R_1 = 0.0576$ $wR_2 = 0.1499$
Largest difference peak and hole (e Å^{-3})	0.418 and -0.442

complexes [7] (Scheme 1). The study of the structure–magnetic properties relationship on this type of materials revealed that the existence of a 1D $\cdots D^+A^-D^+A^-D^+A^-\cdots$ chain structure, clearly favored ferromagnetic coupling [3].

In case of [Fe(Cp*)$_2$]TCNQ, depending on the preparation method three different phases could be isolated, a paramagnetic (α) [8], a metamagnetic (β) [1], and a ferromagnetic (γ) [6a]. The metamagnetic and ferromagnetic phases presented very similar structures, based on the alternated linear $\cdots D^+A^-D^+A^-D^+A^-\cdots$ chain motive, with slight differences on the intra and interchain arrangements [6a]. The magnetic behavior in these compounds is dominated by intrachain DA ferromagnetic interactions and the different magnetic behavior of β and γ phases is due to existence of weak interchain antiferromagnetic (AFM) interactions in case of the β phase compound.

In spite of the difficulty in anticipating magnetic properties due to the difficulties of controlling the crystal structure, as the polymorphism in [Fe(Cp*)$_2$]-TCNQ is a good example, acceptors such as TCNQ or DCNQI seem to be good candidates to be used in the design of molecular materials exhibiting predictable magnetic properties. Since slight structural modifications can be induced through these acceptors, with the use of different substituents on the four free positions of the C_6 rings. This opens perspectives of controlling the intra and interchain arrangements and, as consequently, the magnetic behavior of these ETS.

We report here the synthesis, crystal structure and magnetic behavior of the metamagnet [Fe(Cp*)$_2$]DMe–DCNQI [9].

2. Results and discussion

The salt [Fe(Cp*)$_2$]DMe–DCNQI was prepared by combining equimolar acetonitrile solutions of [Fe(Cp*)$_2$] and DMe–DCNQI, through the transfer of one electron from the donor to the acceptor. Upon mixing the solution changed immediately from yellow to dark blue and a dark blue polycrystalline precipitate was collected after concentrating the solution and standing overnight at −20°C.

[Fe(Cp*)$_2$]DMe–DCNQI crystallizes in triclinic space group $P\bar{1}$, the crystal and experimental data are summarized in Table 1. Fig. 1 shows the molecular diagrams with the atomic numbering scheme, for the cation and the anion. In the asymmetric unit, for both molecules there is only one half and the whole molecule is generated in both cases by a center of symmetry. In the cation the Fe atom is in a special position and, in the anion, the center of symmetry lies in the C_6 ring plane of the molecule.

The [Fe(Cp*)$_2$]$^{\bullet +}$ radical cation has a C_5 local symmetry and the two C_5 rings show a staggered conformation, which is the most common in this type of salts. The average Fe–C, C–C and C–Me Fe–C_5 (Fe–C_5 centroid) distances, 2.093(3), 1.418(5), 1.500(5) and 1.713(8) Å, are in good agreement with the values observed for other salts, as seen in Table 2. The radical anion, DMe–DCNQI$^{\bullet -}$, is planar and the bond lengths and angles observed are in good agreement with those reported for other DMe–DCNQI$^-$ based compounds, $N\equiv C = 1.155(5)$, $N–C = 1.320(5)$, $N=C = 1.353(5)$ (which shows the delocalization on the NCN fragment), $C–C = 1.425(5)$ and 1.428(5) (in the ring), $C=C = 1.3651(5)$ and $C–CH_3 = 1.506(5)$ Å [10].

As in the case of other decamethylferrocenium based electron-transfer salts with planar polynitrile acceptors (TCNQ [6a,11], DDQ [12], C_3CN_5 [13]...), for [Fe(Cp*)$_2$]DMe–DCNQI the crystal structure consists on a parallel arrangement of 1D chains of alternated radical donors, [Fe(Cp*)$_2$]$^{\bullet +}$, and acceptors, DMe–DCNQI$^{\bullet -}$, ···DADADA···, where the stacking axis corresponds to [111]. The intrachain Fe···Fe distance is 10.641 Å, as shown in Fig. 2(a), and the intrachain

Fe···N separations are 6.223 and 7.344 Å. In the structure of [Fe(Cp*)$_2$]DMe–DCNQI, no contacts shorter than sum of van der Waals radii (C–C: 3.2 Å; C–N: 3.1 A) were found, however, intrachain close contacts between the C$_5$ ring from the donor and the C$_6$ ring from the acceptor were observed, with a C···C distances ranging from 3.552 to 3.672 Å, the distance between the C$_5$ and C$_6$ centroids is 3.617 Å. The angle between the stacking axis and the C$_5$ ring from [Fe(Cp*)$_2$]$^{\bullet +}$ is 92.0°, and the angle between the plane of the radical anions and the stacking axis is 91.7°. The dihedral angle between the C$_5$ ring and the acceptor plane is 2.77° and the distance between the two planes is 3.565 Å. The intrachain Fe–Fe and C$_5$–acceptor distances from

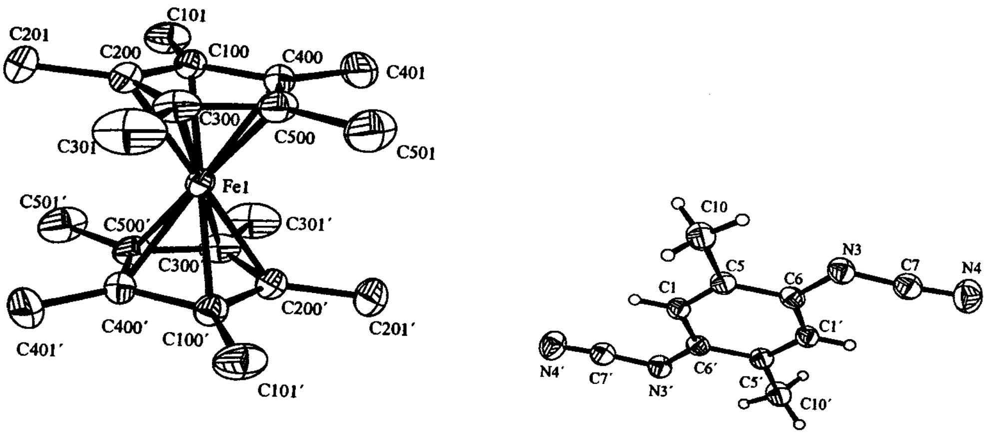

Fig. 1. ORTEP III diagrams of both cation and anion with the atomic labeling scheme. Thermal ellipsoids are drawn at 30% probability level (hydrogen atoms from Cp* have been omitted for clarity).

Table 2
Selected distances and angles for ETS based on planar anions and on [Fe(Cp*)$_2$]$^{\bullet +}$

	Fe–C$_5$ [a] (Å)	Fe–C (Å)	C–C (Å)	C–Me (Å)	C$_5$–A (Å)	Fe–Fe [b] (Å)	T (°C)	Ref.
[Fe(Cp*)$_2$]DMe–DCNQI	1.713	2.095	1.419	1.496	3.565	10.641	20	This work
β-[Fe(Cp*)$_2$]TCNQ	1.694	2.096	1.416	1.509	3.544	10.549	−106	[11]
γ-[Fe(Cp*)$_2$]TCNQ [c]	1.713	2.091	1.406	1.505	3.589; 3.583 [d]	10.837	23	[6a]
[Fe(Cp*)$_2$]DDQ	1.712	2.096	1.422	1.505	3.564	10.616	23	[12]
[Fe(Cp*)$_2$]C$_3$(CN)$_5$	1.710	2.095	1.423	1.501	3.44	10.35	−100	[13]

[a] Ring centroid.

[b] Intrachain.

[c] In this compound the C$_5$Me$_5$ rings are in an eclipsed conformation, while in all the others compounds they are staggered

[d] There are two different DA superposition modes, corresponding to C$_5$–C$_6$ ring centroids distances of 4.193 and 3.588 Å, respectively.

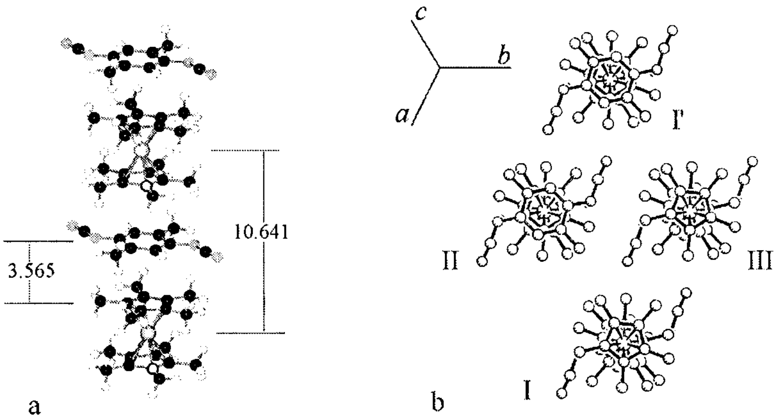

Fig. 2. (a) 1D ···DADADA··· chain in [Fe(Cp*)$_2$]DMe–DCNQI; (b) View normal to the chains (along [111]), showing the three unique chains, I, II and III (hydrogen atoms were omitted for clarity).

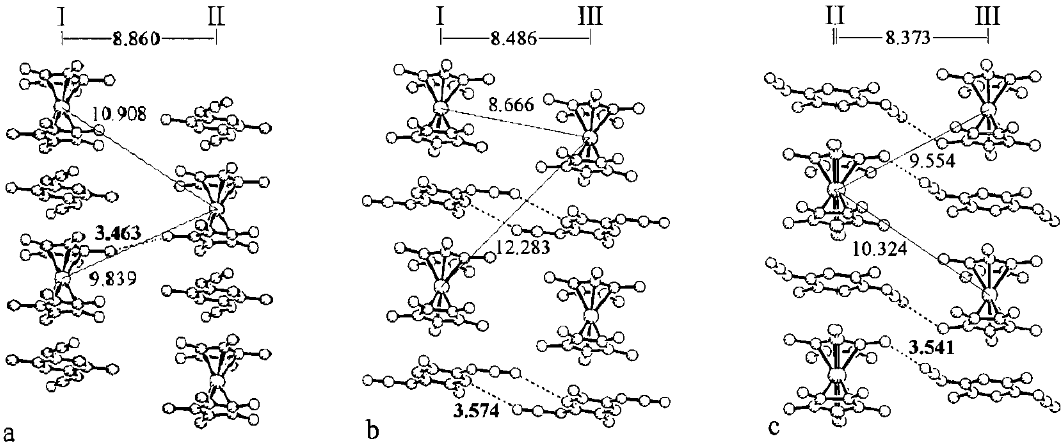

Fig. 3. (a) Out-of-registry arrangement of chains I–II and; (b) in-registry arrangement of chains I–III; (c) out-of-registry arrangement of chains II–III. The solid lines show the interchain separations and the closest interchain M–M distances. The thick dotted lines show the closest interchain interionic distances (hydrogen atoms were omitted for clarity).

[Fe(Cp*)$_2$]DMe–DCNQI are compared with the ones from other decamethylferrocenium based ETS in Table 2.

In the unit cell there are three distinct chains, shown in Fig. 2(b), displaying three unique interchain arrangements, I–II and II–III, which are out-of-registry, and I–III that has an in-registry arrangement. The interchain separations are 8.860, 8.373 and 8.486 Å, for the I–II, II–III and I–III pairs, respectively. Fig. 3 shows these arrangements, along with the shortest distances between the metal centers from different chains and the closest interchain interionic contacts (in bold). For the out-of-registry pairs, the shortest interchain Fe···Fe distances are 9.839 and 10.908 Å for I–II and 9.554 and 10.324 Å for II–III. For the in-registry pair I–III the shorter interchain Fe···Fe distances are 8.666 and 12.283 Å.

Since the magnetic ordering is a bulk property, the interchain interactions are as important as the intrachain interactions and this information is essential in order to understand the spin–spin interactions that dominate the magnetic behavior. For [Fe(Cp*)$_2$]DMe–DCNQI, although no interchain contacts shorter than the sum of the van der Waals radii were detected, relatively short, DA and AA, interionic interchain distances were observed. In the I–II pair the shortest distance (3.463 Å) corresponds to C···C contacts, from the methyl groups of the donors Me$_5$C$_5$ fragments, as shown in Fig. 3(a). In the I–III pair, the shortest interionic interchain distance (3.574 Å) corresponds to N···C contacts from acceptors in different chains, involving the N from the CN group and one of the C from the C$_6$ ring as shown in Fig. 3(b). In the pair II–III the closest interchain contact corresponds to C···C contacts involving one Me group from the donor and a CN group from the acceptor. These interchain contacts are expected to play an important role on the magnetic behavior of the compound, although they are clearly outnumbered by the intrachain contacts. The interchain contacts correspond to interionic distances of the same order of the intrachain contacts, and, in the I–II pair, the DD C···C contacts are even shorter than the intrachain C···C distances. The I–III pair contacts, C···N (3.574 Å) and N···N (3.939 Å), are expected to be determinant in the magnetic interchain interactions, as in this case the N atoms involved are expected to carry most of the spin density from the acceptors. The magnetic interactions between the other pairs of chains involve Me groups, where a quite small spin density is expected, and are expected to be much weaker.

The magnetic susceptibility temperature dependence was obtained by the Faraday method, with an applied magnetic field of 5 kG, and down to temperatures of the order of 20 K, the magnetic susceptibility of [Fe(Cp*)$_2$]DMe–DCNQI follows the Curie–Weiss law, $\chi = C/(T-\theta)$, with a θ value of 3 K. The observed room temperature effective magnetic moment, μ_{eff}, 3.2μ_B, agrees reasonably with the expected value, 3.1μ_B, calculated from $\langle g \rangle = 2.8$ for [Fe(Cp*)$_2$]$^+$ [14] and $\langle g \rangle = 2.0$ for DMe–DCNQI$^-$. The temperature dependence of the χT product is shown in Fig. 4, χT increases upon cooling, as expected for dominant FM interactions.

At low temperatures, for [Fe(Cp*)$_2$]DMe–DCNQI the field-cooled magnetization behavior was observed to be field dependent. As shown in Fig. 5, for low applied fields the magnetization presents a maximum, which for $H = 1.5$ kG occurs at 3.7 K, indicating an AFM transition. Increasing the field the maximum shifts for lower temperatures and at higher applied fields this maximum is suppressed, which is typical of a metamagnetic behavior. The Néel temperature could be determined by ac susceptibility, as the real part, χ', shows a peak at 3.9 K, as it is possible to observe in inset of Fig. 5.

This could be confirmed by the magnetization isothermals sigmoidal behavior observed for [Fe(Cp*)$_2$]DMe–DCNQI, below $T_N = 3.9$ K, as shown in Fig. 6. At 1.7 K, the critical field, defined as the maximum of dM/dH, is $H_C = 5.5$ kG. The inset of Fig. 6 shows the 1.7 K isothermal and the magnetization reaches a value of $1.6N\mu_B$ at 70 kG, which is still lower than the saturation magnetization, $M_{sat} = 2.44N\mu_B$. This situation is typical of linear chain metamagnets, in case the temperature is not far below T_N and the applied magnetic field is not much larger than H_C [15].

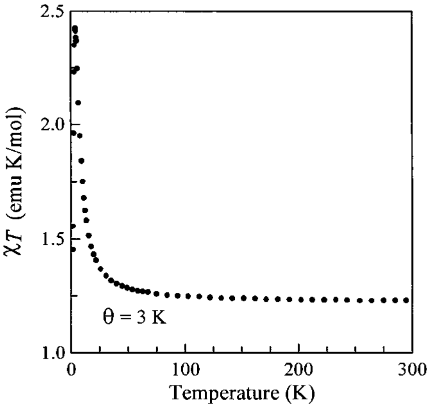

Fig. 4. χT temperature dependence for [Fe(Cp*)$_2$]DMe–DCNQI.

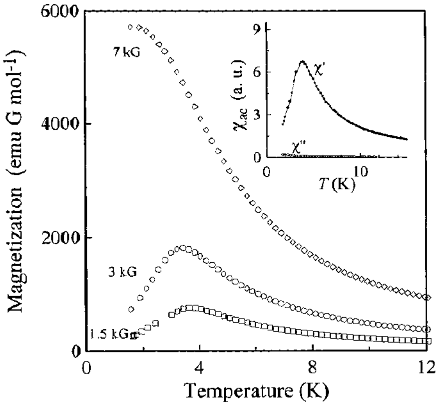

Fig. 5. Magnetization temperature dependence for [Fe(Cp*)$_2$]DMe–DCNQI, with applied magnetic fields of 1.5, 3 and 7 kG. The inset shows the temperature dependence of the real (χ') and imaginary (χ'') parts of χac, at low temperatures.

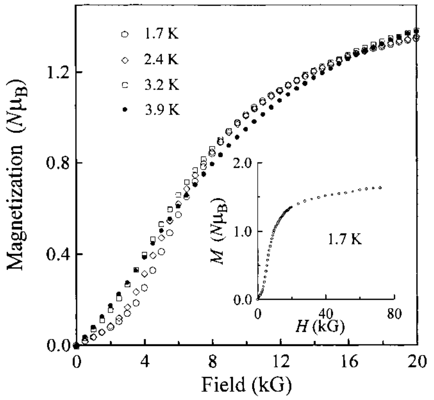

Fig. 6. Magnetization isotherms, for [Fe(Cp*)$_2$]DMe–DCNQI, at 1.7, 2.4, 3.2 and 3.9 K. The inset shows 1.7 K isothermal up to 70 kG.

The metamagnetic behavior of [Fe(Cp*)$_2$]DMe–DCNQI is attributed to the magnetic anisotropy due to the coexistence of strong DA intrachain FM interactions, through the DA $C_6 \cdots C_5$ contacts, with weak interchain AFM interactions. As mentioned before, the AA N···N interchain (I–III pair) must be the most relevant interchain contacts and, admitting that DMe–DCNQI$^{\bullet -}$ presents a spin distribution similar to TCNQ [11], an AFM interaction is expected, as in this case the spin density would have the same sign in both atoms. For the same reason the interchain DD Me···Me contacts (I–II pair) are also expected to lead to AFM interactions.

In Table 3 a summary of the most relevant magnetic parameters of [Fe(Cp*)$_2$]DMe–DCNQI are presented together with selected examples of ETS based on planar anions and on [Fe(Cp*)$_2$]$^{\bullet +}$. Compound **5**, has a $S = 0$ acceptor, $C_3CN_5^-$, and the paramagnetism is due only to the donors, in this case weak DD AFM interactions give rise to the small and negative θ value. With the exception of **3**, which presents a different intrachain DA arrangement (conformation of the C_5Me_5 rings and DA stacking mode), in the other compounds a reasonable correlation can be observed between the observed θ values and the C_5–acceptor (C_5–A) and Fe–Fe distances. Due to the structural similarities this correlation would be expected to hold in some extent in these compounds, as the intrachain DA interactions are based on similar C_5–C_6 contacts. However, the correlation must be considered with some reserves, as it is sensitive to the particular superposition mode of the C_6 and C_5 rings, and to the spin densities on the atoms from those rings. Which are expected to be affected by the substituents, in case of the acceptor, or by the conformation of the C_5Me_5 rings, in the case of the donor. As in case of **2** the structural data were obtained at −100°C, the distances were corrected, considering the thermal contraction observed in compound **4** [16]. The values obtained for C_5–A and Fe–Fe distances are 3.576 and 10.644 Å. The θ values increase in the order $\mathbf{2} \approx \mathbf{1} < \mathbf{3} < \mathbf{4}$, while the C_5–A distances decrease in the order $\mathbf{3} > \mathbf{2} \geq \mathbf{1} > \mathbf{4}$ and Fe–Fe in the order $\mathbf{3} > \mathbf{2} \approx \mathbf{1} > \mathbf{4}$.

The metamagnets [Fe(Cp*)$_2$]DMe–DCNQI (**1**) and β-[Fe(Cp*)$_2$]TCNQ (**2**), although not isostructural, present a very similar solid state structure. In the alternated linear DA chains, the intrachain Fe–Fe distance present similar values, 10.641 Å for **1** and 10.549 Å for **2** (10.644 Å with thermal contraction correction), and the interchain arrangements are also very similar. However, the interchain distances were observed to be

Table 3
Summary of θ values, critical temperatures, and fields for ETS based on planar anions and on $[Fe(Cp^*)_2]^{\bullet +}$

	S_A [a]	θ (K)	M. Ord. [b]	T_C (K)	H_C (G [c])	Ref.
1 $[Fe(Cp^*)_2]$DMe–DCNQI	1/2	3.1	MM	3.9	5500	This work
2 β-$[Fe(Cp^*)_2]$TCNQ	1/2	3	MM	2.55	1600	[1]
3 γ-$[Fe(Cp^*)_2]$TCNQ	1/2	3.8	FM	3.0		[6a]
4 $[Fe(Cp^*)_2]$DDQ	1/1	10.3	[d]			[12]
5 $[Fe(Cp^*)_2]C_3(CN)_5$	0	−1.2	[d]			[13]

[a] Acceptor spin value.

[b] Magnetic ordering.

[c] Critical field.

[d] No magnetic ordering.

shorter in case of **1**, in-reg: 8.486; out-of-reg.: 8.373 and 8.860 Å, as compared to compound **2**, in-reg: 8.573; out-of-reg.: 8.447 and 9.362 Å (with thermal contraction correction, in-reg: 8.616; out-of-reg.: 8.481 and 9.399 Å). From the crystal structure analysis of these compounds a similar DA intrachain magnetic coupling, J_{DA}, would be expected since, the Fe–Fe intrachain separations and C_5–acceptor distances observed for **1** and **2** (corrected for temperature) are similar. The intrachain coupling must be stronger in case of **1**, as the intrachain separations in this compound are shorter. Besides the the AA N···N interchain distances (from the in-registry pairs) are considerably shorter in case of **1** (3.939 Å) than for **2** (4.080 Å or with thermal correction 4.100 Å). This is consistent with the higher critical temperature observed for **1**, as $T_N \propto |E_{intra}E_{inter}|^{1/2}$ [6c], where the intrachain DA interaction, $E_{intra} \propto S_D S_A J_{DA}$, and E_{inter} is the effective interchain interaction.

In the study of the metamagnetic transitions in linear chain compounds [17], a simple Ising model was used, with an intrachain and two interchain constants, and, according to that model, for those compounds the metamagnetic critical fields are proportional to the interchain exchange constants. In case of the metamagnetic compounds, $[Fe(Cp^*)_2]$DMe–DCNQI (**1**) and β-$[Fe(Cp^*)_2]$TCNQ (**2**), the critical field in case of **1** ($H_C = 5.5$ kG) is larger than the observed for **2** ($H_C = 1.6$ kG) confirming that the AFM interchain interactions are considerably stronger in the case of compound **1**.

As in β-$[Fe(Cp^*)_2]$TCNQ, the in-registry AFM interchain interactions seem to be determinant in the metamagnetic behavior of $[Fe(Cp^*)_2]$DMe–DCNQI. A considerable weakening of those interactions could be obtained through the introduction of bulkier substituents in DCNQI, and in this way it could lead to the stabilization of a FM ground state. The bulkier substituents could even induce different interchain arrangements, as in γ-$[Fe(Cp^*)_2]$TCNQ, where no similar in-registry interchain arrangements are observed, thus favoring the existence of bulk FM.

3. Summary

The crystal structure of the electron-transfer salt $[Fe(Cp^*)_2]$DMe–DCNQI, is based on an array of parallel alternating donor/acceptor ···DADADA··· stacks. At high temperatures, the magnetic behavior is dominated by strong DA FM intrachain interactions, and at low temperatures it exhibits a metamagnetic behavior, due to the coexistence of weaker (DD and AA) AFM intrachain interactions. The crystal structure and magnetic behavior of $[Fe(Cp^*)_2]$DMe–DCNQI is compared with other ETS based on decamethylferrocene and on polynitrile planar acceptors, based on a similar alternated linear chain motive, in particular with the metamagnet β-$[Fe(Cp^*)_2]$TCNQ, which presents a very similar crystal structure. The higher values of T_N and H_C in case of $[Fe(Cp^*)_2]$DMe–DCNQI, are assigned essentially to stronger interchain AFM interactions in this salt. This work suggests that bulk FM can be achieved by the introduction of bulkier substituents on the acceptor, in order to weaken the AFM in-registry interchain arrangement interactions or eventually to suppress that type of arrangements.

4. Experimental

4.1. General remarks

Commercially available starting material, decamethylferrocene (Aldrich), was used without further purification and *N*,*N*′-dicyano-2,5-dimethyl-1,4-benzoquinonediimine was prepared as described in the literature [18]. Acetonitrile and dichloromethane were distilled over P_2O_5, under nitrogen, and deaerated either by successive alternated freezing and evacuating cycles or by bubbling argon for ca. 30 min. *n*-Pentane and *n*-hexane were distilled over sodium and deaerated by successive alternated freezing and evacuating cycles. All the syntheses were carried out under nitrogen or argon, in gloveboxes or using schlenk techniques. Elemental analyses were carried out on a Carlo Erba (EA 1110-CHNS-O).

4.2. [Fe(Cp)$_2$]DMe–DCNQI*

It was prepared from the addition of a warm 7 ml acetonitrile solution of 36.0 mg (0.195 mmol) of DMe–DCNQI to a warm 15 ml acetonitrile solution of 64.0 mg (0.196 mmol) of [Fe(Cp*)$_2$]. With mixing the (yellow) solutions turned dark blue. The mixture was concentrated by partial evaporation of the solution to ca. 2 ml volume and was left overnight at ≈ -20°C, 32.8 mg (64 mmol) of a dark blue crystalline precipitate, with a 33% yield, was collected by vacuum filtration and washed with pentane. Anal. Found (Calc.) for $C_{20}H_{30}FeC_{10}N_4H_8$: C, 70.32 (70.58); H, 7.89 (7.50); N, 10.60 (10.97)%. Dark blue platted shaped crystals of [Fe(Cp*)$_2$]DMe–DCNQI suitable for X-ray analysis were obtained, at room temperature, by slow diffusion of [Fe(Cp*)$_2$] and DMe-DCNQI, in a three compartment cell, using a mixture of acetonitrile + dichloromethane + *n*-hexane (1:2:30) as solvent.

4.3. Magnetic characterization

Magnetic susceptibility data of [Fe(Cp*)$_2$]DMe–DCNQI polycrystalline samples, using a teflon sample holder, were obtained with an Oxford Instruments Faraday system, between 1.8 and 300 K. Compressed polycrystalline samples were used in order to minimize orientation effects. Low temperature magnetization temperature and field dependences were obtained with an Oxford Instruments Magnetometer (MagLab System 2000), between 1.6 and 12 K, by an extraction method. Ac susceptibility measurements were also obtained with the MagLab system. Magnetization data were corrected for contributions due to sample holder and core diamagnetism, estimated from tabulated Pascal constants.

4.4. X-ray crystallographic study

A single crystal of [Fe(Cp*)$_2$]DMe–DCNQI with the approximate dimensions of $0.21 \times 0.15 \times 0.09$ mm^3 was used for X-ray data collection on a Enraf Nonius CAD4 diffractometer, with graphite monochromated Mo–K$_\alpha$ radiation ($\lambda = 0.71069$ Å), at room temperature. Data was corrected for Lorentz polarization, linear decay (no decay was detected) and empirically for absorption (ψ scans). The structure was solved by a combination of direct methods and difference Fourier synthesis. All non-hydrogen atoms were refined anisotropically and hydrogen atoms were inserted in calculated positions riding on the parent C atoms, isotropic temperature factors $U(\mathrm{H}) = 1.5U_{\mathrm{eq}}(\mathrm{C})$. All calculations were done using SHELXS-97 [19] and SHELXL-97 [20]. Molecular and crystal representations were obtained with ORTEP III [21] and SCHAKAL-97 [22]. A summary of the crystal data and refinement procedures is given in Table 1.

5. Supplementary material

Crystallographic data (excluding structure factors) for the structural analysis have been deposited with the Cambridge Crystallographic Data Centre, CCDC no. 157884. Copies of this information may be obtained from The Director, CCDC, 12 Union Road, Cambridge CB2 1EZ, UK (fax: +44-1233-336-033; e-mail: deposit@ccdc.cam.ac.uk or www: http://www.ccdc.cam.ac.uk).

Acknowledgements

This work was partially supported by 'Fundação para a Ciência e Tecnologia' under contract PRAXIS/P/QUI/12603/1998 from PRAXIS XXI program.

References

[1] J.A. Candela, L.J. Swartzendruber, J.S. Miller, M.J. Rice, J. Am. Chem. Soc. 101 (1979) 2755.

[2] J.S. Miller, J.C. Calabrese, A.J. Epstein, W. Bigelow, J.H. Zhang, W.M. Reiff, J. Chem. Soc. Chem. Commun. (1986) 1026.

[3] J.S. Miller, A.J. Epstein, in: C.J. O'Connor (Ed.), Research Frontiers in Magnetochemistry, World Science Publishers, Singapore, 1993, p. 283.

[4] J.S. Miller, A.J. Epstein, in: E. Coronado, P. Delhaès, D. Gatteschi, J.S. Miller (Eds.), Molecular Magnetism: from Molecular Assemblies to the Devices, Kluwer Academic Publishers, Dordrecht, 1996, p. 379.

[5] (a) G.T. Yee, J.M. Manriquez, D.A. Dixon, R.S. McLean, D.M. Grosky, R.B. Flippen, K.S. Narayan, A.J. Epstein, J.S. Miller, Adv. Mater. 3 (1991) 309;
(b) D.M. Eichhorn, D.C. Skee, W.E. Broderick, B.M. Hoffman, Inorg. Chem. 32 (1993) 491;
(c) J.S. Miller, R.S. McLean, C. Vasquez, F. Zuo, A.J. Epstein, J. Mater. Chem. 3 (1993) 215.

[6] (a) W.E. Broderick, D.M. Eichhorn, X. Liu, P.J. Toscano, S.M. Owens, B.M. Hoffman, J. Am. Chem. Soc. 117 (1995) 3641;
(b) W.E. Broderick, J.A. Thompson, E.P. Day, B.M. Hoffman, Science 249 (1990) 401;
(c) W.E. Broderick, B.M. Hoffman, J. Am. Chem. Soc. 113 (1991) 6334.

[7] (a) V. Gama, D. Belo, S. Rabaça, I.C. Santos, H. Alves, J.C. Waerenborgh, M.T. Duarte, R.T. Henriques, Eur. J. Inorg. Chem. (2000) 2101;
(b) W.E. Broderick, J.A. Thompson, B.M. Hoffman, Inorg. Chem. 30 (1991) 2958;
(c) V. Gama, S. Rabaça, C. Ramos, D. Belo, I.C. Santos, M.T. Duarte, Mol. Cryst. Liq. Cryst. 335 (1999) 81.

[8] A.H. Reis Jr, L.D. Preston, J.M. Williams, S.W. Peterson, G.A. Candela, L.J. Swartzendruber, J.S. Miller, J. Am. Chem. Soc. 101 (1979) 2756.

[9] The synthesis and magnetic properties of a compound with a similar composition was reported before, but its ground state was not clearly established, and the crystal structure was not reported: J.S. Miller, C. Vazquez, R.S. McLean, W.M. Reiff, S. Hunig, Adv. Mater. 5 (1993) 448.

[10] (a) A. Aumuller, P. Erk, E. Hadicke, K. Peters, H.G. von Schnering, Chem. Ber. 124 (1991) 2001;

(b) S. Hunig, M. Kemmer, H. Meixner, K. Sinzger, H. Wenner, T. Bauer, E. Tillmanns, F.R. Lux, M. Hollstein, H.-G. Groß, U. Langohr, H.-P. Werner, J.U. von Schutz, H.-C. Wolf, Eur. J. Inorg. Chem. (1999) 899.

[11] J.S. Miller, J.H. Zhang, W.M. Reiff, D.A. Dixon, L.D. Preston, A.H. Reis Jr, E. Gebert, M. Extine, J. Troup, A.J. Epstein, M.D. Ward, J. Phys. Chem. 91 (1987) 4344.

[12] E. Gebert, A.H. Reis Jr, J.S. Miller, H. Rommelmann, A.J. Epstein, J. Am. Chem. Soc. 104 (1982) 4403.

[13] J.S. Miller, J.C. Calabrese, H. Rommelmann, S.R. Chittipeddi, J.H. Zhang, W.M. Reiff, A.J. Epstein, J. Am. Chem. Soc. 109 (1987) 769.

[14] J.S. Miller, J.C. Calabrese, A.J. Epstein, Inorg. Chem. 28 (1989) 4230.

[15] E. Stryjewski, N. Giordano, Adv. Phys. 26 (1977) 487.

[16] In the compound $[Fe(Cp^*)_2]$DDQ (see Ref [3]), the values obtained at 23°C, relative to the ones obtained at −70°C, present an increase of ca 0.9% in the Fe–Fe intrachain separation and ca. 0.5 and 0.4% in the in-registry and out-of-registry interchain distances, respectively. An increase of the order of 0.6–0.7% was observed in the out-of-registry interchain contacts.

[17] A. Narath, Phys. Rev. 139 (1965) A 1221.

[18] A. Aumuller, S. Hunig, Liebigs Ann. Chem. (1986) 142.

[19] G.M. Sheldrick, Acta Crystallogr. Sect. A 46 (1990) 467 direct methods (SHELXS-97).

[20] G.M. Sheldrick, SHELXL-97, A computer program for refinement of crystal structures, University of Göttingen; G.M. Sheldrick, T.R. Schneider, SHELXL: high-resolution refinement, Methods Enzymol. (Macromol. Crystallogr. Part B, C.W. Carter, R.M. Sweet, Eds.), 277 (1997) 319.

[21] M.N. Burnett, C.K. Johnson, ORTEP III: Oak Ridge thermal ellipsoid plot program for crystal structure illustrations, Oak Ridge National Laboratory Report ORNL-6895, 1996.

[22] E. Keller, SCHAKAL-97, a computer program for the representation of molecular and crystallographic models, Kristallographisches Institut der Universität Freiburg i. Br., Germany, 1997.